Two-dimensional vibrational lineshapes of amide III, II, I and A bands in a helical peptide

Tomoyuki Hayashi, Shaul Mukamel *

Department of Chemistry, University of California, Irvine, California 92697-2025, USA

ARTICLE INFO

ABSTRACT

An effective exciton Hamiltonian for all amide bands is used to calculate the absorption and photon echo spectra of a 17 residue helical peptide (YKKKH17). The cross peak bandshapes are sensitive to the inter-band couplings. Fluctuations of the local amide frequencies of the all amide fundamental and their overtone and combination states are calculated using the multipole electric field induced by environment employing the electrostatic DFT map of N-methyl acetamide. Couplings between neighboring peptide units are obtained using the anharmonic vibrational Hamiltonian of glycine dipeptide (GLDP) at the BPW91/6-31G(d,p) level. Electrostatic couplings between non-neighboring units are calculated by a fourth rank transition multipole coupling (TMC) expansion including $1/R^3$ (dipole–dipole), $1/R^4$ (quadrupole–dipole), and $1/R^5$ (quadrupole–quadrupole and octapole–dipole) interactions.

© 2008 Elsevier B.V. All rights reserved.

1. Introduction

The amide III, II, I and A vibrational modes of proteins have infrared absorption [1,2] around 1200 cm^{-1}, 1500 cm^{-1}, 1700 cm^{-1}, and 3500 cm^{-1}, respectively. These vibrations are localized on the amide bonds. Their sensitivity to hydrogen bonding, dipole–dipole interactions and peptide backbone geometry provides useful indicators of secondary-structural changes [3–7]. The amide I and A are mainly the CO and N–H bond stretch, respectively. The amide II and III bonds are mixtures of the C–N stretch and H–N–C bend. Coherent ultrafast infrared spectroscopy has been applied to probe protein structure [8–10]. Two-dimensional infrared cross peaks of amide I with other amide modes (A and II) have been reported in model systems of the amide bond [11–13]. Recent simulations [14] showed that the cross peak bandshapes are sensitive to the correlated hydrogen bond dynamics at the two atom sites where the two amide vibrations reside. This makes them most suitable for probing the local protein environment. The amide A vibration is not resolved in the infrared due to the overlapping broad absorption of water. The cross peaks thus provide a direct window into this vibration.

Most simulation effort had so far focused on the highly-localized amide I vibrations [15–20] which are the easiest to model. Ab initio calculations of all amide band normal modes have been reported [21,22]. The peptide force field depends on frequencies of the local

amide vibrations as well as their couplings between neighboring and non-neighboring amide units. Torii and Tasumi had constructed a map of amide I couplings between neighboring amide units based on Hartree–Fock calculations of a glycine dipeptide (GLDP) for various Ramachandran angles (ψ and ϕ) [15]. They also calculated the amide I couplings between non-neighboring amide units using the transition dipole coupling mechanism (TDC). Neighboring amide I maps have subsequently been developed [23,18] based on normal mode calculations of GLDP at higher computational levels (MP2 and DFT) by employing the Hessian reconstruction. Non-neighboring couplings were calculated by the interaction of vibration-induced partial charges determined by normal mode analysis of NMA [18]. Side-chain contributions to the amide I frequencies of β-hairpins have been investigated as well [19,20]. Hydrogen-bonding with the surrounding water was found to affect the amide I local mode frequencies. All of these studies are restricted to the amide I mode and neglect the anharmonic character of the inter-unit couplings as well as contributions of inter-amide couplings to the diagonal and off-diagonal anharmonicity of the amide modes.

We have developed an electrostatic DFT map (EDM) [24,25] that includes the fundamental, the diagonal and off-diagonal anharmonic frequency fluctuations of all amide states in NMA. The map provides a first-principles effective vibrational Hamiltonian which includes the fundamental, overtone, combination frequencies and transition moments of the amide III, II, I and A. It is based on vibrational eigenstate calculations of 6th order anharmonic DFT potentials in the presence of up to 3rd rank multipole (octapole) electric fields. Higher multipoles of the electric field make significant contributions to the frequency

* Corresponding author.
   E-mail address: smukamel@uci.edu (S. Mukamel).

fluctuations and line broadening [24]. The EDM reproduces the experimental amide I and II anharmonicities [13].

Couplings between neighboring peptide units are obtained using a quartic anharmonic vibrational DFT potential of glycine dipeptide (GLDP) at the BPW91/6-31G(d,p) level for various Ramachandran angles. Electrostatic model is used for couplings between non-neighboring units. We have expanded the transition charge density couplings (TCDC) in multipoles including $\sim R^{-3}$ (dipole–dipole), $\sim R^{-4}$ (dipole–quadrupole), $\sim R^{-5}$ (quadrupole–quadrupole and dipole–octapole) interactions. The higher order multipoles were found critical for smaller R for the relatively delocalized bending amide modes (II and III). These are usually neglected [15,18]. The couplings were expanded as bilinear products of local amide modes(LAMs) of the two sites, by neglecting the electronic anharmonicities.

The peptide Hamiltonian was expanded in a basis of Local Amide States (LAS); the eigenstates of the local Hamiltonian which consist of the localized amide III, II, I and A. These include the fundamental and their overtone and combination states (14 states per each site). The coupling matrix elements are calculated between all amide fundamentals, overtones, and combinations localized in neighboring and non-neighboring peptide units. The LAS anharmonicities contribute to the anharmonicities in these couplings, which are included in the calculations.

2. The simulation protocol

The anharmonic vibrational Hamiltonian of the peptide was expanded in the form.

$$
\begin{aligned}
\hat{H} = &\sum_m \left(\sum_i \frac{p_{mi}^2}{2M_{mi}} + \sum_{k=1}^{6} \sum_{i_1,\ldots,i_k} f_{i_1\ldots i_k}^{(k)}(\boldsymbol{C}) \prod_{a=1}^{k} q_{mi_a} \right) \\
&+ \sum_{m,n}^{|m-n|=1} \sum_{k=2}^{4} \sum_{k'=1}^{k-1} \sum_{i_1,\ldots,i_k} J_{mn,i_1\ldots i_k}^{(k,k')}(\phi,\psi) \prod_{a=1}^{k'} q_{mi_a} \prod_{b=k'+1}^{k} q_{ni_b} \\
&+ \sum_{m,n}^{|m-n|>1} \sum_{i,j} K_{mn,ij} q_{mi} q_{nj}
\end{aligned}
\tag{1}
$$

Here q_{mi} represent the 5 local amide modes (LAM) of the amide site m and M_{mi} and p_{mi} are their masses and momentums. The first term

Fig. 1. Structure of 17 residue helical peptide (YKKKH17) [26].

representing the local amide sites is expanded up to 6th order in the local amide modes (LAMs). The anharmonic force field $f_{i_1\ldots i_k}^{(k)}$ depends on the fluctuating multipole electric field $\boldsymbol{C} \equiv (E_x, E_y, E_z, \ldots, E_{xxx}, E_{yyy}, E_{zzz}, \ldots)$ generated by the other parts of the protein and water, it is calculated based on the electrostatic DFT map of the NMA [25] combined with a MD trajectory. The second term represents the couplings between the neighboring amide units, expanded to 4th order in LAMs. Neighboring couplings are obtained by electronic structure calculations of glycine dipeptide (GLDP), parametrized with respect to the Ramachandran angles ϕ and ψ. The last term includes the Coulombic couplings between non-neighboring units and approximated by the transition multipole couplings up to 4th rank. They are bilinear in LAMs of the two sites.

The Hamiltonian was first diagonalized by neglecting all inter-unit couplings (only the first term in Eq. (1) is included) to generate the 14 local amide states (LAS) per amide unit (4 amide fundamentals, 4 overtone, and 6 combinations). The effective vibrational Hamiltonian is finally recast using the LAS.

$$
\hat{H} = \sum_a \hbar\omega_{ma}(\boldsymbol{C}) \hat{B}_{ma} \hat{B}_{ma}^\dagger + \hat{H}_{\text{neighbor}} + \hat{H}_{\text{non-neighbor}}
\tag{2}
$$

$$
\hat{H}_{\text{neighbor}} = \sum_{m,n}^{|m-n|=1} \sum_{a,b} J_{mn,ab}(\phi,\psi) \hat{B}_{ma} \hat{B}_{nb}^\dagger
\tag{3}
$$

$$
\begin{aligned}
\hat{H}_{\text{non-neighbor}} = &\sum_{m,n}^{|m-n|>1} \left\{ \sum_{a,b} K'_{mn,ab} \left(\hat{B}_{ma}^\dagger \hat{B}_{nb} + \hat{B}_{ma} \hat{B}_{nb}^\dagger + \hat{B}_{ma} \hat{B}_{nb} + \hat{B}_{ma}^\dagger \hat{B}_{nb}^\dagger \right) \right. \\
&+ \sum_{a,b,c} K''_{mn,abc} \left(\hat{B}_{na}^\dagger \hat{B}_{nb} \hat{B}_{mc} + \hat{B}_{na}^\dagger \hat{B}_{nb} \hat{B}_{mc}^\dagger \right) \\
&\left. + \sum_{a,b,c,d} K'''_{mn,abcd} \hat{B}_{ma}^\dagger \hat{B}_{mb} \hat{B}_{nc}^\dagger \hat{B}_{nd} \right\}
\end{aligned}
\tag{4}
$$

where $\hat{B}_{ma}$ and $\hat{B}_{ma}^\dagger$ are the Pauli exciton creation and annihilation operators for to the transition between the ground state and the LAS ma. 14×16 creation and annihilation operators are defined in total. Couplings between non-neighboring amide units were expressed to quartic order in $\hat{B}_{ma}$ and $\hat{B}_{ma}^\dagger$.

We have calculated the eigenstates of this effective anharmonic Hamiltonian and simulated the infrared bands of the amide III, II, I and A and three-pulse photon echo signals of the amide I and all 4 amide cross peak regions of a 17 residue helical peptide Ac-YAAKAAAAKAAAAKAAH-NH2 (YKKKH17) (Fig. 1) in water. Since YKKKH17 is small and preserves its helical structure in water, it is a good candidate for investigating the 2D photon echo signatures of the amide couplings. We have used the MD trajectory of a one YKKKH17 and 4330 H_2O molecules as reported in Ref. [26]. Four chloride ions were added to make the system neutral. CHARMM27 [27] and TIP3 force fields were used with a 12 Å cut-off of the Lennard–Jones interactions and the Ewald sum of the electrostatic interactions. The CHARMM package [27] was used and a 1 ns trajectory was sampled with 1 fs time step.

The eigenstates of each snapshot were calculated by expansion in Hartree products of LAS. Since YKKKH17 has 16 amide units and each amide unit has 15 LAS (ground state, +14 states), the basis set is $|\psi\rangle = |a_1\rangle |a_2\rangle \ldots |a_{16}\rangle$ ($a_i = 0, \ldots, 14$). The eigenstates were calculated by numerical diagonalization of the Hamiltonian. The sum over states expressions and the SPECTRON code [26] were used to simulate the spectra. These were averaged over 100 snapshots and a 5.5 cm^{-1} homogeneous linewidth was added to all transitions.

3. Results and discussion

The vibrational couplings between the amide states in different amide units are shown in Fig. 2. The couplings of the amide I fundamental neighboring units are always positive, since their transition dipoles are parallel. Amide I couplings between non-neighboring
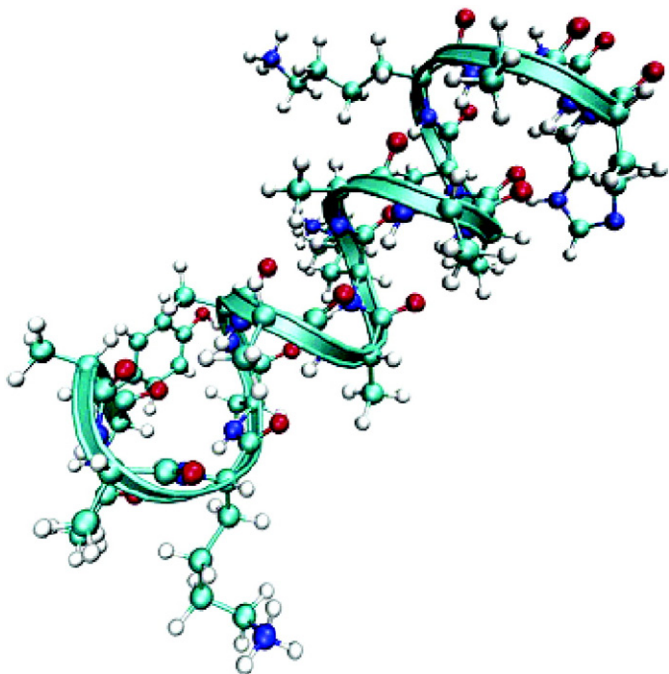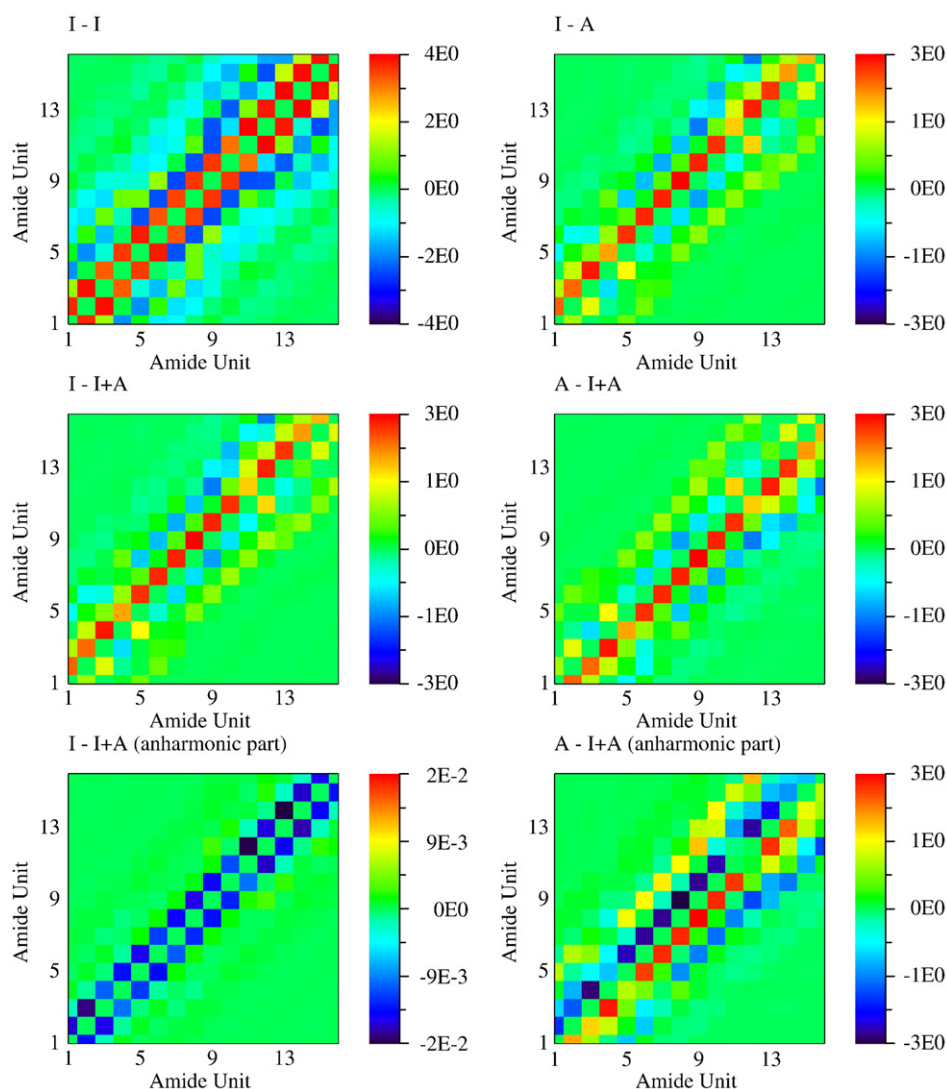
Fig. 2. Vibrational couplings between local amide states. sinh($J_{mn,ab}$) of Eq. (3) in cm^{-1}.

units are negative since the two dipoles have close to head-to-tail configurations due to the peptide helical structure. The coupling patterns of amide I–A fundamentals are similar to amide I–I couplings, but are weaker due to the smaller transition dipole moment of amide A. The couplings between the amide I or amide A fundamentals and amide I+A combination states show a different pattern.

For a single MD snapshot the 16 eigenstates around 1700 cm^{-1} are mostly linear combinations of 16 local amide I fundamental states. 16 eigenstates in the 3500 cm^{-1} frequency region come from local amide A fundamental states. The contributions of each local amide vibration to these eigenstates obtained from 3 snapshots are shown in Fig. 3. The Amide I eigenstates are delocalized over 3 to 5 amide bonds. YKKKH17 has bulky residues (tyrosine and histidine) on the both terminals and rather compact residues (mostly alanine with a few lysine) in the middle. The peptide has a α-helical structure on the both terminal, but a 3_{10}-helical structure between residues 4 and 11. In the 3_{10}-helical part the hydrogen bondings are formed between n and $n+3$ residues which cause strong couplings between the units separated by 3. The α-helical part has the hydrogen bondings between n and $n+4$ residues resulting in couplings between units separated by 4 amino acids. The amide I eigenstates are thus delocalized along the helical axis rather than the peptide backbone. The amide A eigenstates are more localized

on 1 to 2 neighboring amide bonds since their transition dipole moments are smaller and have different directions from amide I. The amide I fundamental eigenstates are more delocalized than the amide A. This may be attributed to the larger transition dipole moments.

The simulated absorption lineshapes of the amide III, II, I and A regions are shown in Fig. 4. All amide modes have a single peak and a almost symmetric bandshape except for the amide A which has a lower frequency tail. This stems from a helical structure of the peptide which results in a homogeneous environment for all amide units. The amide II intensity is weaker than the amide I, which is consistent with experiment. However the simulated amide II bandwidth is narrower and its peak height is higher than experiment, which is ascribed to that the amide II frequency fluctuation of NMA is underestimated due to insufficient electrostatic sampling ([25]) resulting in the narrower amide II bandwidth. The amide A has the broadest band due to the large local amide A frequency fluctuation (Fig. 8 of Ref. [25]). This may be rationalized since the weaker N–H bond is strongly affected by the hydrogen bond formation with water.

The photon echo cross peaks of the amide I and the amide III, II, I and A are displayed in Fig. 5 (Eq. (5.20), (5.23) and (5.24) in Ref. ([28])). The absolute value spectra of the 4 cross peaks are
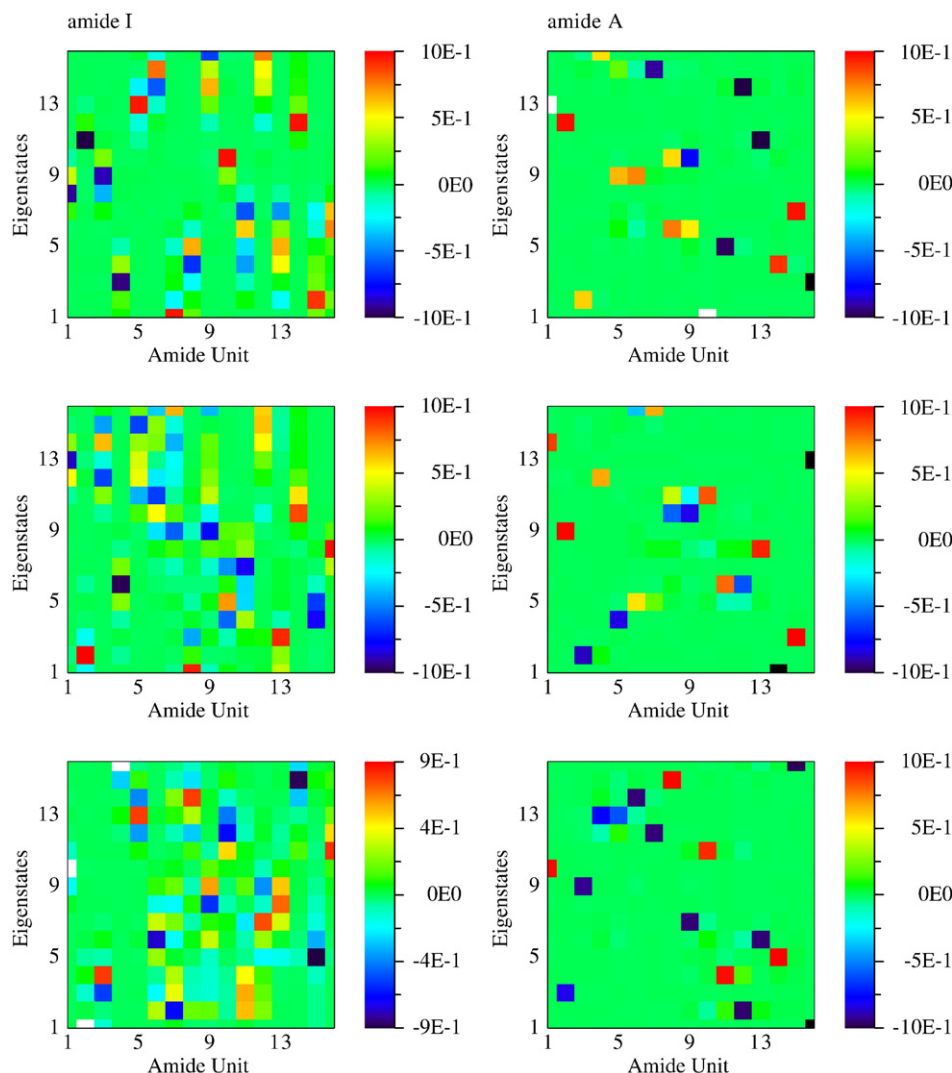
Fig. 3. Contributions of each amide bond to the 16 eigenstates of amide I and A fundamental states obtained from three MD snapshots.

featureless due to the helical structure except that the I–III cross peak region has double peaks in ω_3 direction and the I–I cross peak has a weak subband. The band width along the ω_1 and ω_3 direction corresponds to the inhomogeneous frequency distribu-
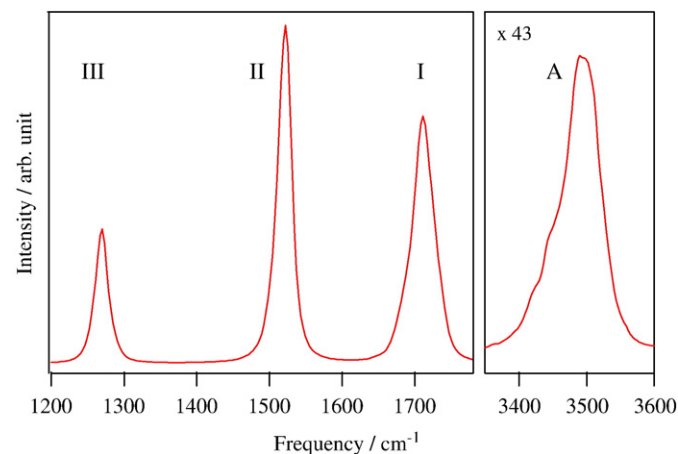

Fig. 4. Simulated linear absorption of the amide I, II, III and A.

tions of the amide I and the 4 amide modes. The imaginary (absorptive) parts of the signals have more structure. Unlike NMA [14] where positive excited state absorption and negative ground state bleach peaks have similar intensities in a given cross peak, the negative peaks here are stronger. The negative peaks involve the two pairs of the transitions between the ground state and the amide fundamental states and the orientational averages of the product of these IR transition dipoles moments contributing to the signals are always positive [28]. The combination states give positive peaks and the product of the transition dipole moments can be negative due to the anharmonicities. The negative peaks from different pathways accumulate to form the strong peaks. Positive peaks from different Liouville space paths may cancel out. It should be noted that lifetime broadening could also contribute to the cross peak bandshapes and is expected to broaden more the positive excited state absorption peak. This effect is not included in the present simulation.

To investigate the bandshape sensitivity to the couplings between the amide modes in different amide units, the amide I–III, I–A cross peaks and the amide I–I diagonal peak were also calculated by turning off these couplings. Comparison with the original calculations is shown in Fig. 6. The positive peaks of all I–III, I–I and I–A regions are stronger when the couplings are
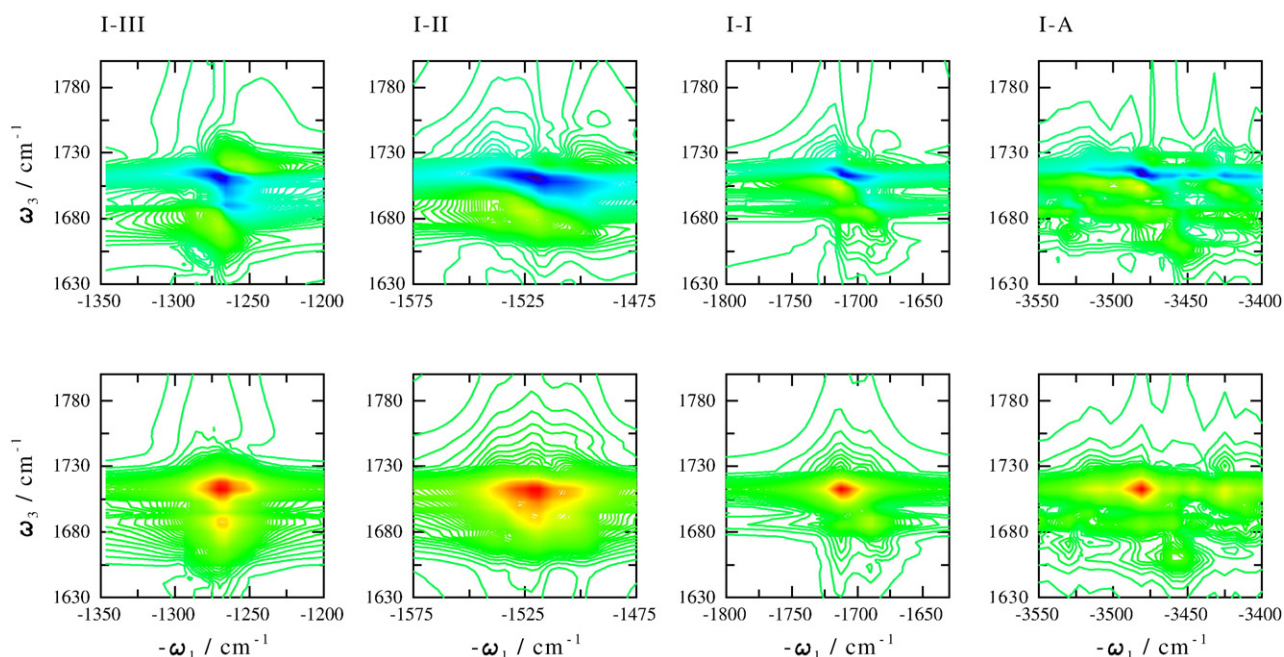
Fig. 5. Photon echo cross peaks of the amide I and all 4 amide modes. Top: imaginary part; bottom: absolute value amplitude. Calculations made using Eq. (5.20), (5.23) and (5.24) in Ref. ([28]).
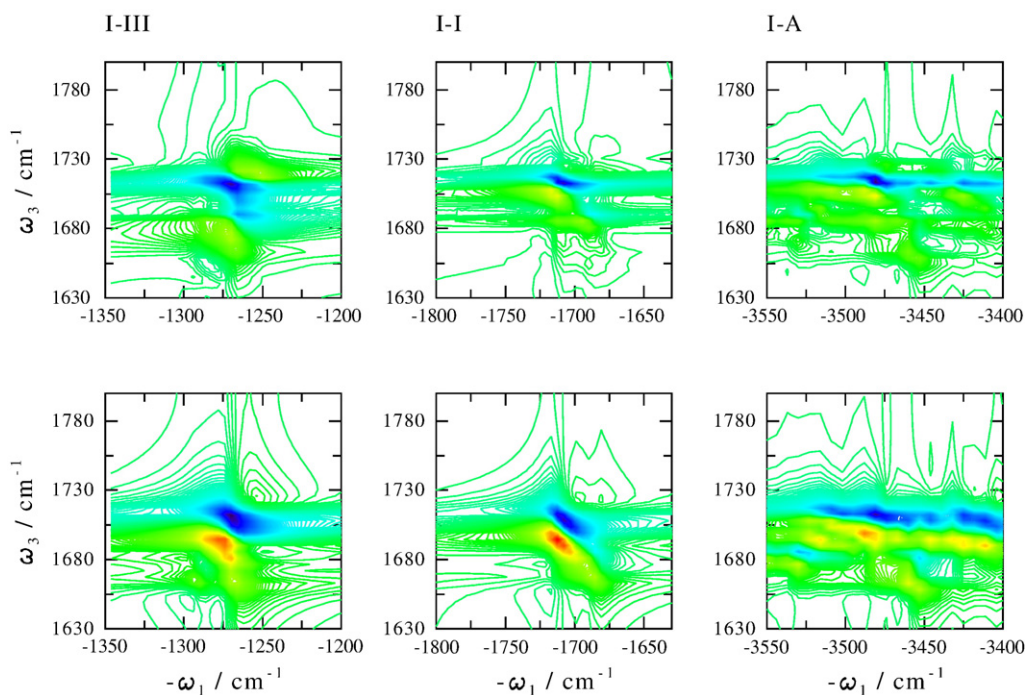

Fig. 6. Photon echo cross peaks with (top) and without (bottom) amide couplings between different amide units, as indicated.

switched off. The amide I–I bandshapes significantly depends on the couplings. Both negative and positive peaks are more elongated in the diagonal direction when the couplings are switched off.

References

[1] T. Miyazawa, T. Shimanouchi, S.I. Mizushima, J. Chem. Phys. 29 (1958) 611.
[2] M. Tsuboi, T. Onishi, I. Nakagawa, T. Shimanouchi, S. Mizushima, Spectrochim. Acta 12 (1958) 253.
[3] H. Torii, M. Tasumi, J. Chem. Phys. 96 (1992) 3379.
[4] H. Torii, M. Tasumi, Infrared Spectroscopy of Biomolecules, Wiley-Liss, New York, 1996.
[5] D.M. Byler, H. Susi, Biopolymers 25 (1986) 469.
[6] W.K. Surewicz, H.H. Mantsch, Biochim. Biophys. Acta 952 (1988) 115.
[7] M. Jackson, P.I. Haris, D. Chapman, J. Mol. Struct. 214 (1989) 329.
[8] S. Mukamel, Annu. Rev. Phys. Chem. 51 (2000) 691.
[9] R.M. Hochrasser, Proc. Natl. Acad. Sci. U. S. A. 104 (2007) 14189.

[10] R.M. Hochstrasser, Proc. Natl. Acad. Sci. U. S. A. 104 (2007) 14190.
[11] I.V. Rubtsov, J. Wang, R.M. Hochstrasser, J. Chem. Phys. 118 (2003) 7733.
[12] I.V. Rubtsov, J. Wang, R.M. Hochstrasser, Proc. Natl. Acad. Sci. 100 (2003) 5601.
[13] L.P. DeFlores, Z. Ganim, S.F. Ackley, H.S. Chung, A. Tokmakoff, J. Phys. Chem. B 110 (2006) 18973.
[14] T. Hayashi, S. Mukamel, J. Chem. Phys. 125 (2006) 194510.
[15] H. Torii, M. Tasumi, J. Raman Spectrosc. 29 (1998) 81.
[16] A.M. Moran, S.M. Park, S. Mukamel, J. Chem. Phys. 118 (2003) 9971.
[17] P. Bour, T.A. Keiderling, J. Chem. Phys. 119 (2003) 11253.
[18] T.L. Jansen, A.G. Dijkstra, T.M. Watson, J.D. Hirst, J. Knoester, J. Chem. Phys. 125 (2006) 044502.
[19] S. Hahn, S. Ham, M. Cho, J. Phys. Chem. B 109 (2005) 11789.
[20] H. Lee, S.S. Kim, J.H. Choi, M. Cho, J. Phys. Chem. B 109 (2005) 5331.
[21] S.H. Lee, S. Krimm, Biopolymers 46 (1998) 283.
[22] J. Kubelka, R. Huang, T.A. Keiderling, J. Phys. Chem. B 109 (2005) 8231.
[23] R.D. Gorbunov, D.S. Kosov, G. Stock, J. Chem. Phys. 122 (2005) 224904.
[24] T. Hayashi, T.L. Jansen, W. Zhuang, S. Mukamel, J. Phys. Chem. A 109 (2005) 64.
[25] T. Hayashi, W. Zhuang, S. Mukamel, J. Phys. Chem. A 109 (2005) 9747.
[26] W. Zhuang, D. Abramavicius, T. Hayashi, S. Mukamel, J. Phys. Chem. B 110 (2006) 3362.
[27] B.R. Brooks, R.E. Bruccoleri, B.D. Olafson, D.J. States, S. Swaminathan, M. Karplus, J. Comput. Chem. 4 (1983) 187.
[28] S. Mukamel, D. Abramavicius, Chem. Rev. 104 (2004) 2073.